Plane-Intersection Reconstruction of Integrated Point Clouds toward Property Valuation-Oriented 3D Building Models

Ratri Widyastuti[1], Deni Suwardhi[1], Andri Hernandi[1], Darren A.P. Siagian[2], Arnadi Murtiyoso[3], Fabio Remondino[4]

[1]Spatial System and Cadastral Research Group, Institut Teknologi Bandung (ITB), Indonesia – (ratri, deni.suwardhi, andri.hernandi)@itb.ac.id
[2] Geodesy & Geomatic Eng. Undergraduate Programme, Institut Teknologi Bandung (ITB), Indonesia - 15122021@mahasiswa.itb.ac.id
[3]Université de Strasbourg, CNRS, INSA Strasbourg, ICube Laboratory UMR 7357, Photogrammetry and Geomatics Group, 67000, Strasbourg, France– arnadi.murtiyoso@insa-strasbourg.fr
[4]3D Optical Metrology (3DOM) Unit, Bruno Kessler Foundation (FBK), Trento, Italy – remondino@fbk.eu

Keywords: 3D Property Valuation, 3D Building Models, 3D Cadastre, Fiscal Cadastre, High Level of Detail (LoD).

Abstract

Three-dimensional (3D) building models with a high level of geometric and semantic detail are increasingly required to support fiscal cadastral applications, such as property valuation and taxation. In dense urban environments, however, the availability of complete and high-quality 3D data remains limited, particularly for exterior wall information. This research proposes a rule-based 3D building reconstruction workflow using integrated Unmanned Aerial Vehicle-Light-Detection and Ranging (UAV-LiDAR) and terrestrial handheld scanner point clouds to generate building models with hanging roofs and explicit building elements. The proposed method combines region growing segmentation for roof and exterior wall extraction, planar surface reconstruction through plane fitting, and geometric primitive intersection to construct roof meshes and building envelopes. Roof geometry is reconstructed from planar roof components, while exterior wall points are used to adjust the building envelope and support hanging roof modelling. The resulting 3D building model is represented as separated elements, including roof, exterior walls, and floor surfaces, enabling element-based area calculation and cost estimation for fiscal cadastral purposes. Quantitative evaluation using point cloud-to-model distance analysis shows that the reconstruction accuracy falls within the commonly reported range for Level of Detail 2 (LoD2) building models, despite limitations caused by segmentation precision and parameter sensitivity of rule-based algorithms. The results demonstrate that the proposed approach provides a feasible solution for 3D building modelling in environments with incomplete data, while supporting transparent and assessment-oriented fiscal cadastral workflows.

1. Introduction

In many developing countries, there is an increasing need for a three-dimensional (3D) cadastral system that provides high Level of Detail (LoD) building models to support fiscal cadastral functions such as taxation and property valuation. Accurate geometric dimensions and model details directly affect valuation precision. As demonstrated by Yamani et al. (2021), deriving 3D variables such as building envelope geometry, roof slopes, and façade details significantly improves the modelling accuracy of property values. Furthermore, 3D building models enhance transparency in property valuation, as Kara et al. (2023) utilized large-scale 3D building models to perform city-wide assessments efficiently and transparently.

However, converting raw 3D data sources into detailed 3D building models requires a high degree of automation. Recent developments have shifted toward non-rule-based approaches, particularly Artificial Intelligence (AI) in computer vision, to automate segmentation and classification of point clouds. Deep Learning (DL) approaches such as fully convolutional networks (FCN), PointNet, PointNet++, dynamic graph convolutional neural networks (DGCNN), and KPConv have demonstrated strong performance in segmenting point clouds. However, their effectiveness heavily depends on the availability and quality of training data, while Machine Learning (ML) methods, although more broadly applicable, still tend to introduce unavoidable noise in the segmentation results (Widyastuti et al., 2024; Grilli et al., 2023; Kim et al., 2020; Phan et al., 2018; Qi et al., 2017; Thomas et al., 2019). This situation occurs in several countries that have limited 3D data sources. Geometric features in ML approaches for segmenting point clouds provide advantages in addressing this problem (Widyastuti et al., 2025).

Although many point cloud segmentation approaches have been developed using non-rule-based AI, 3D building reconstruction automation still needs to be further developed. The plane-intersection method has been widely applied for 3D building reconstruction, as it can overcome problems associated with incomplete point cloud data. Plane-intersection–based building reconstruction has evolved from general polygonal surface recovery toward city-scale reconstruction. PolyFit establishes a foundational paradigm that extracts planar primitives from point clouds, generates candidate faces from plane intersections, and selects an optimal subset via global optimization to produce compact polygonal surfaces. Although it produces clean and lightweight planar geometry, it can become computationally heavy when the number of candidates increases because the algorithm constructs to evaluate all plane candidates, and it remains sensitive to missing or poorly segmented planes (Nan & Wonka, 2017). City3D addresses a key PolyFit limitation related to missing façade evidence in airborne LiDAR by introducing building-specific reasoning, most notably wall hypotheses inferred from roof structures and additional constraints, thereby improving robustness for urban Aerial Laser Scanning (ALS) scenes. However, it still inherits assumptions of vertical walls and may struggle with highly irregular or fine architectural details (Huang et al., 2022).

Recent watertight reconstruction approaches extend plane-intersection paradigms by enforcing topological closure through plane-set and half-space formulations (Kaufhold & Kada, 2025).

https://doi.org/10.5194/isprs-archives-XLVIII-2-W12-2026-503-2026 |

However, their tendency toward simplified roof geometry and surface-only representations indicates the need for hybrid learning–geometry frameworks to achieve detailed and volumetric 3D building reconstruction. To overcome this limitation, Wang et al. (2023) introduced the Building 3D dataset and benchmarks, shifting the focus from plane-based surface closure to data-driven learning of roof structural complexity at the urban scale. By representing roofs as wireframes composed of corners and edges, their deep learning–based framework enables the modelling of more complex and irregular roof configurations that are difficult to capture with plane-intersection or half-space approaches. However, the framework focuses exclusively on roof structures without explicitly modelling roof–wall relationships or volumetric building representations.

The experimental results described earlier indicate that edge reconstruction remains challenging under incomplete and noisy point cloud conditions, often leading to missing or fragmented edges, which can be addressed using plane–roof intersection methods. In addition, the resulting models are not constructed using the exterior walls available in the data but are instead generated from roof edges, meaning that the possibility of roof overhangs is not modelled. Moreover, the resulting 3D models do not separate surface elements for roofs, ceilings, exterior walls, and floors, which are important for 3D property valuation using the cost estimation method by calculating the cost of work multiplied by the area of the building elements (Tokla & Subsomboon, 2020)

In conclusion, this research discusses how to produce a 3D building model composed of explicit building elements for assessment purposes, including a roof suspended from partially available exterior wall point clouds and complex roof structures. The aim of this research is to produce a 3D building model using a planar intersection approach for fiscal cadastral purposes, in which a building envelope with a hanging roof is constructed. By explicitly modelling building components such as the roof, walls, ceiling, and floor, the resulting 3D building model supports element-based representation that is useful for 3D property valuation in fiscal cadastre.

2. Methodology

Basic concepts of this research, which are used in the flow diagram in Figure 1, are described as follows:

a. Region Growing
This algorithm is used because it has advantages in individual roof segmentation, where the modelling starts within one land parcel, as in cadastral practice. One land parcel may contain more than one building; therefore, this algorithm is advantageous in such cases. When the curvature parameter is set differently based on the segmentation purpose, this algorithm can be used to fulfil two purposes of roof segmentation: individual roofs within one parcel and roof components within a single roof (Widyastuti et al., 2025).

b. Concave Hull (Yahya et al., 2017)
Concave Hull is applied when a point set does not require a convex space but instead allows concave shapes, enabling the formation of interior angles between points without exceeding 180°, thereby better representing the actual geometry of the data (Yahya et al., 2017). In this research, the Concave Hull technique is adopted to extract polygon boundaries by controlling the degree of concavity and node excavation distance, allowing flexible boundary formation while preserving geometric validity.

c. Plane Fitting (Surface Reconstruction)
This process finds a mathematical plane that best represents a set of 3D points. The equation of the plane is shown in Equation (1).

$$Ax + By + Cz + D = 0 \quad (1)$$

where A, B, and C are the components of the normal vector of the plane. To find the plane equation, Singular Value Decomposition (SVD) is used. First, the mean of the 3D points is computed as Equation (2).

$$\bar{P} = \frac{1}{n}\sum P_i \quad (2)$$

where P_i represents (x_i, y_i, z_i) and n is the number of the points. Then, the covariance matrix is computed based on the mean of the 3D points. Then, the covariance matrix is computed based on the mean of the 3D points. The normal vector n of the best-fitting plane is the eigenvector corresponding to the smallest eigenvalue of the covariance matrix.

d. Geometric Primitive Intersection
The purpose of this concept is to find line or point intersections between planes, or between a plane and a line. The equation of a line is shown in Equation (3).

$$L(t) = L_0 + tV \quad (3)$$

where L_0 is starting point, V is the direction vector, and t represents the position along the line. The line of intersection between two planes is obtained from the cross product of their normal vectors, provided that $\|n_1 \text{ x } n_2\| \neq 0$, or equivalently when the dot product satisfies $|n_1.n_2| < 1$. The cross product of the two plane normals yields the line direction vector V. Point intersections can also be determined as follows:

- Line–plane intersection: to find the point on a line that intersects a plane, the parameter t is computed using Equation (4).

  $$t = \frac{(P_0 - L_0).n}{V.n} \quad (4)$$

  Where P_0 is a reference point on the plane
- Three or more planes intersection
  Intersection of three or more planes: the point of intersection P between three planes can be computed using Equation (5).

  $$P = \frac{d_1(n_2 x n_3) + d_2(n_3 x n_1) + d_3(n_1 x n_2)}{n_1.(n_2 x n_3)} \quad (5)$$

Where d_i is the scalar offset from the origin and n_i is the normal vector of each plane. When resolving the intersection of more than three planes, the problem is formulated as an overdetermined linear system. The dot product is used to define the distance of a point to each plane. The optimal vertex is obtained by minimizing the sum of squared residuals using a linear least squares approach, which computes the point that is spatially closest to all participating planes. Plane intersections must have a non-zero scalar triple product.

The initial step of this study involves processing point cloud data acquired from UAV (Unmanned Aerial Vehicle) and handheld scanners. These datasets are integrated through a two-stage registration process within CloudCompare. First, a coarse registration is performed using point-to-point registration (point-pair-based alignment), where at least four natural points are manually identified across both datasets to establish an initial alignment. Subsequently, a fine registration is executed using the Iterative Closest Point (ICP) algorithm to minimize the root mean square (RMS) error and achieve high-precision data fusion. Once the registration is complete, the integrated point cloud is segmented into the roof and exterior wall classes.

Following this, the segmented roof data is used to reconstruct a complete 3D building with a hanging roof through planar segmentation and plane intersection operations (Figure 1). Initially, the raw point cloud undergoes region growing segmentation to isolate planar roof components, a common approach in LiDAR-based roof reconstruction that groups neighbouring points into coherent planar patches based on continuity criteria. These segmented planar patches are used to compute plane intersections where adjacent roof planes meet, yielding line segments that represent roof ridges and edges. Their intersection points provide an initial set of roof boundary vertices, which are continuously refined as additional intersections with boundary representations are introduced. The final set of roof vertices is used to construct a mesh surface via Delaunay triangulation, a well-established method for creating a Triangulated Irregular Network (TIN) that approximates complex surface geometry while preserving vertex connectivity. This roof mesh serves as the topmost surface of the building model. The flow diagram of this research can be seen in Figure 1.

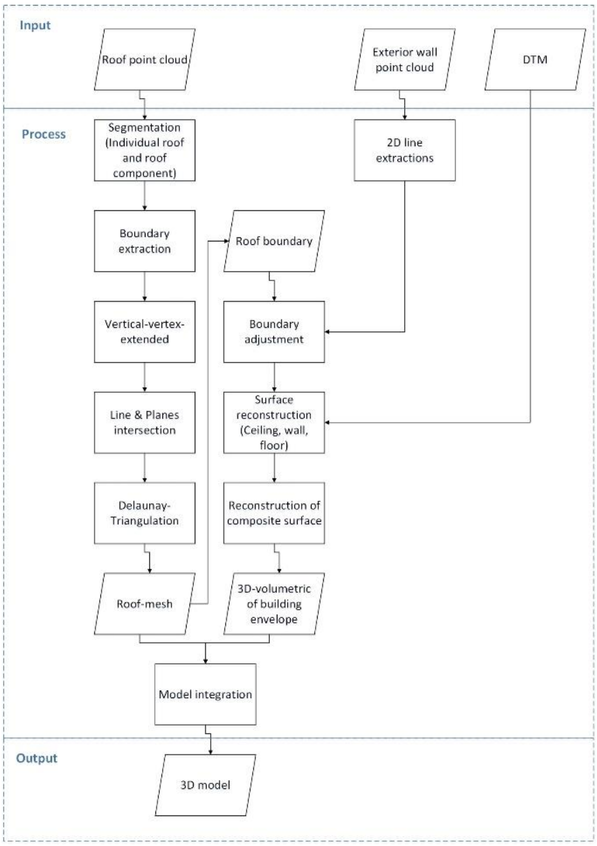

Figure 1. Flow diagram of this research

Building envelopes are constructed using an extrusion-based surface modelling strategy, in which the refined roof boundary is vertically extruded downward to the Digital Terrain Model (DTM) to generate vertical wall surfaces and a triangulated floor surface within the footprint, following established extrusion workflows for surface-based 3D city models (Biljecki et al., 2014). Watertight geometry is ensured by overlaying the updated footprint with the original roof mesh boundary and resolving discrepancies through polygon Boolean difference operations and surface patching, a standard practice in computational geometry and GIS-based solid and surface reconstruction (Oosterom et al., 2005). The resulting geometry is represented as a composite surface composed of roof (ceiling), wall, and ground surfaces, consistent with boundary-surface representations adopted in CityGML and surface-based volumetric modelling of urban objects (Kolbe et al., 2005). Prior to extrusion, roof geometry is derived from point cloud data using planar roof segmentation and planar patch intersection, where region growing is applied to extract coherent roof components, planar primitives are estimated for each segment, and line segments resulting from plane–plane intersections define roof ridges and edges. Such procedures are well established in airborne and mobile LiDAR roof reconstruction literature (B Souza & Amorim, 2012; Yi et al., 2017).

After the 3D building model is formed, the analysis is conducted using point cloud-to-model comparison. Statistical metrics, including maximum distance, mean distance, and standard deviation, are used to evaluate worst-case error, typical error, and the variation or spread of point distances (Patil & Kalantari, 2025). In conclusion, this research applies a combination of region growing, concave hull, plane fitting, and geometric primitive intersection to support the 3D building reconstruction process. Region growing is used to segment individual roofs and roof components, concave hull is applied for roof boundary extraction, plane fitting is employed to construct planar representations of roof components, and geometric primitive intersection is utilized to derive roof boundaries and interior intersection points. Through the integration of these basic concepts, the proposed approach enables the generation of structured roof geometry as a foundation for subsequent building envelope modelling and fiscal cadastral analysis.

3. Results

This section presents the results of the proposed 3D building reconstruction workflow based on integrated UAV-LiDAR and handheld-scanner point clouds. The results are organized to illustrate each major processing stage, including roof segmentation, roof mesh construction, and building envelope modelling. Visual and geometric outputs are provided to demonstrate the effectiveness of the proposed approach in handling complex roof structures and hanging roofs. In addition, quantitative and qualitative comparisons are used to evaluate the resulting models against the original point cloud data.

3.1 Data

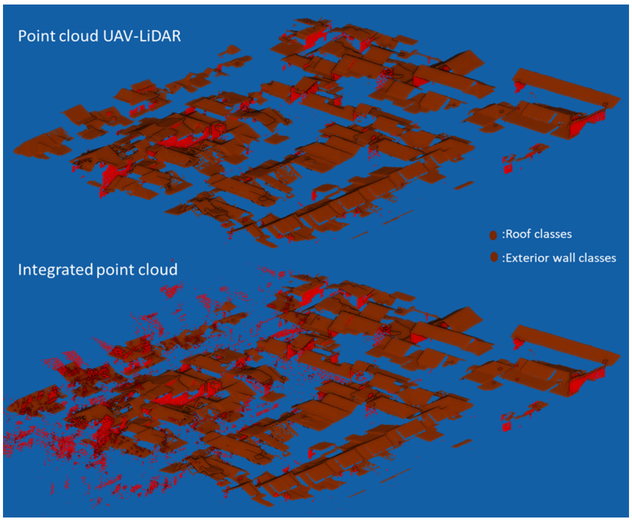

Figure 2. Classified UAV-LiDAR point cloud (top) and classified integrated point cloud (bottom)

The datasets utilized in this research were acquired using Geosun LiDAR technologies, specifically the gAirHawk GS-100C UAV-LiDAR system and the GS-100 handheld scanner. The UAV-LiDAR data, which maintains a precision of 0.025 m, was captured at a flight altitude of 100 m. The integration of these two datasets resulted in a Root Mean Square Error (RMSE) of 1.108 m during the registration process. The primary input for this study is the segmented version of this integrated point cloud, divided into roof and exterior wall classes. As visualized in Figure 2, the handheld scanner data complements the exterior wall classes (shown in red) by providing structural details on the surfaces that were not captured by the UAV-LiDAR, while the roof classes (shown in brown) are predominantly captured by the UAV-LiDAR.

3.2 Constructions of Roof Mesh

The segmented integrated point cloud is processed using the Region Growing algorithm to obtain individual roofs within one parcel and roof components within one roof (Figure 3).

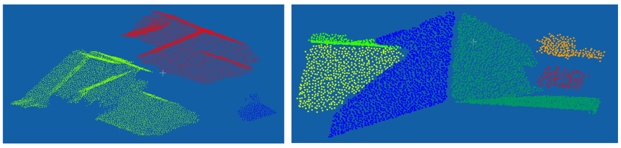

Figure 3. Individual roofs in a parcel (left). Roof components in a roof (right)

The segmented individual roofs are used for boundary extraction, and the roof components are used to construct roof planes. In Figure 4, the left image shows that overlaps and gaps exist between boundaries. These issues must be resolved first by keeping the top roof unchanged. The roof components are then used to construct planar planes (Figure 5).

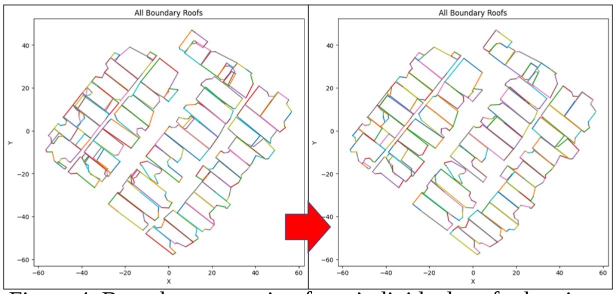

Figure 4. Boundary extraction from individual roofs showing gaps and overlaps (left); boundary adjustment within a parcel (right)

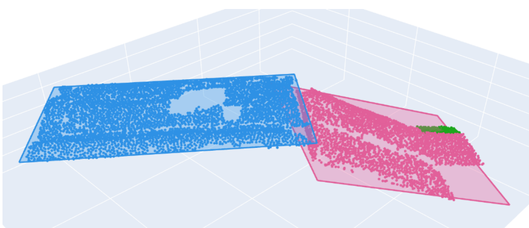

Figure 5. Plane extraction from roof components

The roof planes are used to determine line intersections. Vertices from boundary extraction are used to identify 3D roof intersection points on the roof planes. The 3D roof intersection points are continuously updated through various scenarios. First, the 3D edge boundaries are updated using point intersections obtained from line intersections between planes. Second, the 3D roof intersection points are updated using intersections from line segments inside the 3D roof boundary, resulting in intersection points.

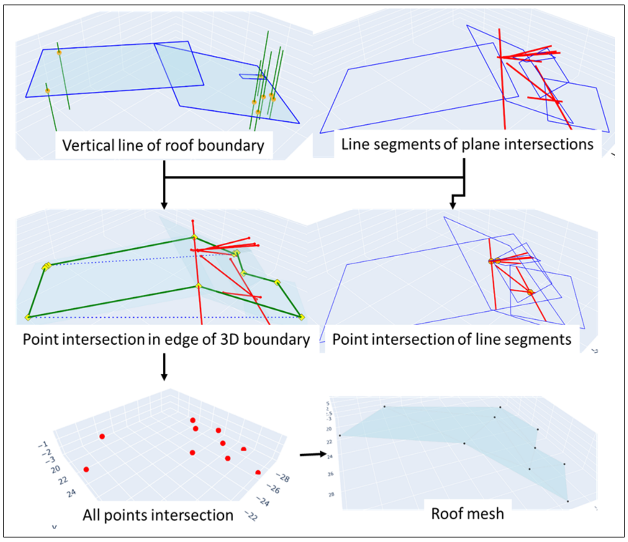

Figure 6. Results of the construction of the roof mesh

Figure 6 shows how the roof mesh construction is obtained. The result of the roof mesh construction can be seen in Figure 7. Table 1 shows the comparison between the point cloud, the mesh model of a 2.5D triangulated surface (height-field–based TIN), and our proposed method.

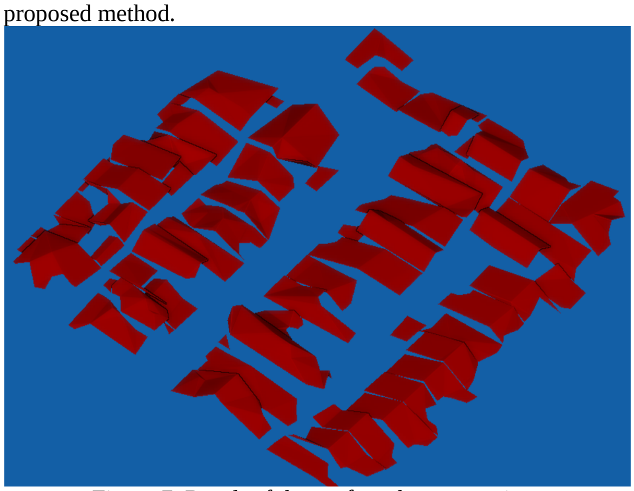

Figure 7. Result of the roof mesh construction

Table 1. The comparison between the point cloud, the mesh model of a 2.5D triangulated surface, and our proposed method.

Point Cloud and Roof Mesh of Ours	Mesh Model
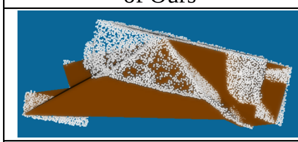	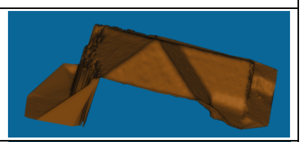
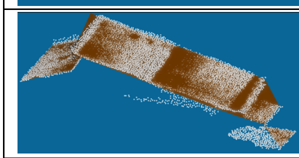	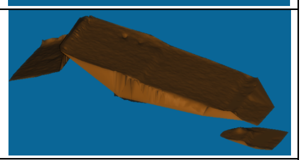
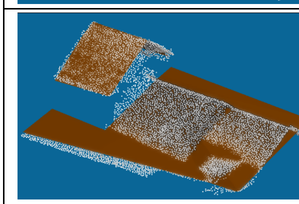	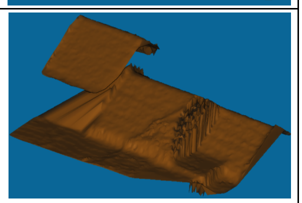

Point Cloud and Roof Mesh of Ours	Mesh Model
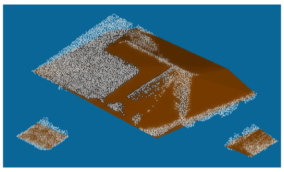	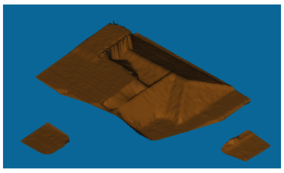
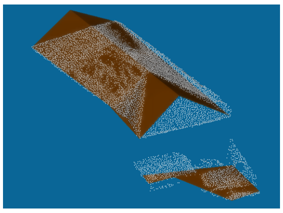	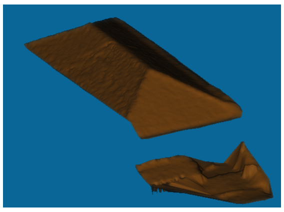
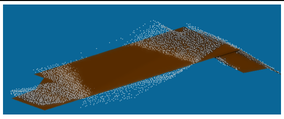	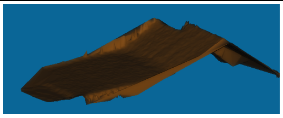

3.3 Constructions of Building Envelope

The roof mesh boundary is used to generate a new 3D boundary, which is adjusted using the segmented point cloud of exterior wall classes. The result of this phase can be seen in Figure 8.

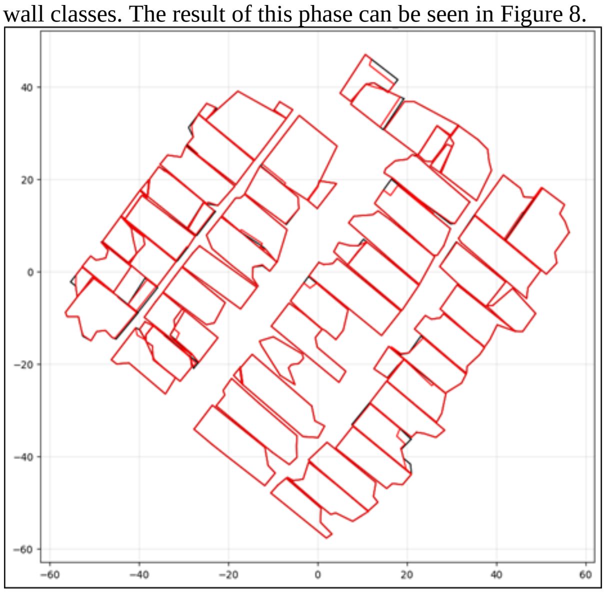

Figure 8. Boundary adjustment results

Figure 8 shows that some segments from the previous boundaries move parallel to the roof boundary. The red segment represents the final boundary of the building envelope, while the black segment represents the original boundary from roof extraction. By using the vertices of the building envelope boundary projected onto the Digital Terrain Model (DTM) and the roof surface mesh model, the final building envelope with a hanging roof is generated, as shown in Figure 9.

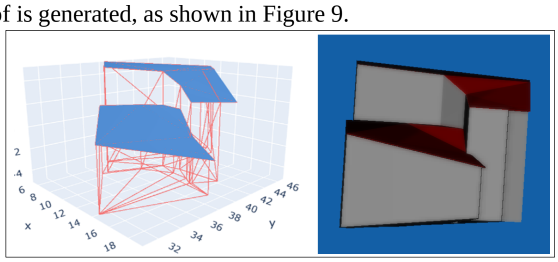

Figure 9. Building envelope with hanging roof

4. Discussion

Even though the 3D reconstruction from segmented point clouds successfully obtained the 3D building envelope with a hanging roof, the quality must be measured using statistics as previously mentioned. Figure 10 shows the graph of the maximum distance between the segmented point cloud and the roof mesh model. Figure 11 shows the visualisation of the highest deviation distance between the segmented point cloud and the roof mesh model. This occurs because the roof component segmentation from the point cloud is not precise. This is a weakness of the rule-based system algorithm, where parameters need to be adjusted according to specific needs (Kang et al., 2019). The weakness of the region growing algorithm is that it is sensitive in determining seeding points and sensitive to the threshold value for grouping points into one groupp (Grilli et al., 2017).

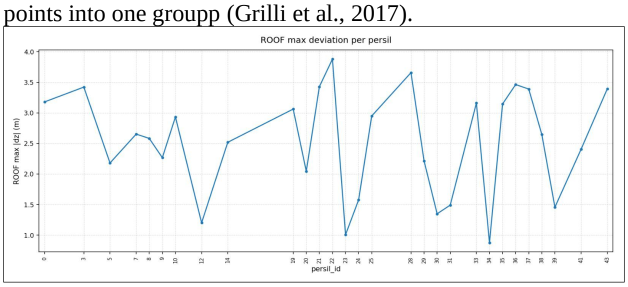

Figure 10. Graph of the maximum distance between the segmented point cloud and the roof mesh model

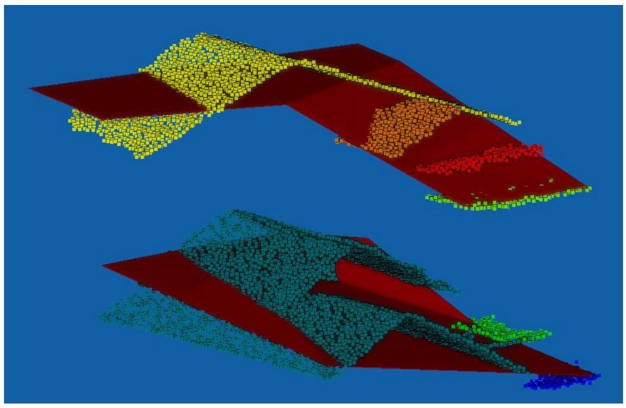

Figure 11. Visualisation of the highest deviation distance between the segmented point cloud and the roof mesh model

The maximum deviation distance can be used to analyse the worst-case error in the 3D model (Patil & Kalantari, 2025). Figure 12 shows the graph of the mean deviation, and the visualisation of the highest mean deviation of the roof model is shown in Figure 13. The statistical mean distance between the segmented point cloud and the roof mesh model shows that the model does not represent the actual geometry well. The highest mean deviation value occurred in parcel 35 in Figure 12. The segmentation of the point cloud into roof components in Figure 13 appears to be smooth. This occurs due to a rule-based algorithm constraint included when constructing the intersection point between the line segment and the roof edge.

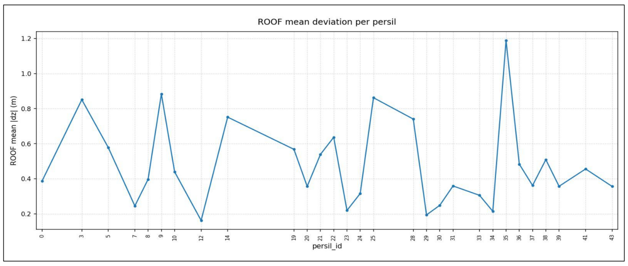

Figure 12. Graph of the mean deviation between the segmented point cloud and the roof mesh model

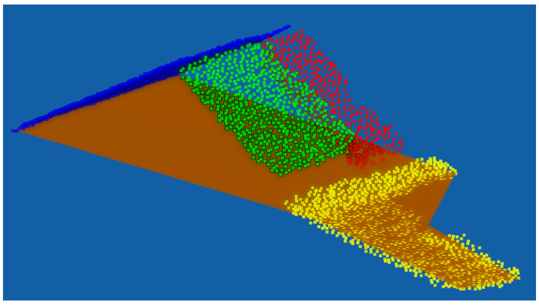

Figure 13. Visualisation of the highest mean deviation of the roof model

The standard deviation of the vertical distance between the point cloud and the roof mesh model is 0.612 m. Although CityGML does not prescribe explicit geometric accuracy thresholds, previous studies on Level of Detail (LoD2) building envelope reconstruction report point-to-model deviations in the range of approximately 0.3–1.0 m, depending on the data source and reconstruction strategy. The obtained standard deviation of 0.6 m therefore falls within the commonly reported accuracy range for LoD2 city-scale building models.

For the exterior wall, the standard deviation between the segmented point cloud and the building envelope is 0.386 m, which is smaller than the deviation for the roof mesh model. However, only a few building envelopes were adjusted to the actual exterior walls derived from the point cloud. In some cases, the standard deviation between the point cloud and the building envelope almost reached the centimetre level. This is caused by the limited number of exterior wall points within a land parcel. Despite the small amount of exterior wall data, the hanging roof could still be constructed using the exterior wall points provided by the integrated point cloud, as shown in Figure 14. The limited exterior point cloud data could help shift the building envelope closer to the actual exterior wall location.

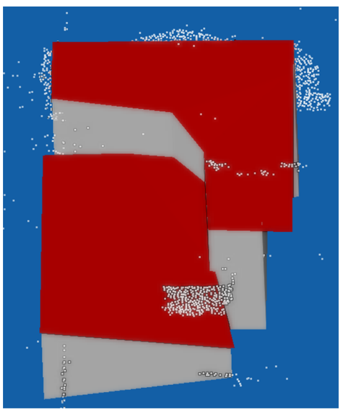

Figure 14. Visualisation of the exterior point cloud with the building envelope

In the exterior wall adjustment section, the results were not optimal due to numerous obstructions, such as cars, fences, and other objects that obstructed data collection. This resulted in many buildings' exterior walls being missed. In addition, the exterior wall adjustment was also affected by a relatively large registration RMSE between the UAV-LiDAR and handheld scanner point clouds. This occurred because the selection of corresponding points for point cloud registration relied on natural features, which introduced greater uncertainty and led to higher registration errors. The actual situation can be seen in the photographs in Figure 15, which are the results of the handheld scanner survey. This approach was chosen because houses are attached to each other, where buildings share roofs, making it difficult to obtain a complete point cloud of a single building. Therefore, an approach that intersects point clouds using parcel boundaries and segments individual roofs within a single parcel is crucial. Furthermore, the increasing variety of housing designs makes roof construction increasingly complex.

Figure 15. Building situation in Indonesia

5. Conclusion

This research demonstrates that 3D building reconstruction using integrated UAV-LiDAR and handheld scanner point cloud data can successfully generate a building envelope with a hanging roof, even under conditions of incomplete exterior wall data. The proposed workflow, which combines region growing segmentation, planar surface reconstruction, and geometric primitive intersection, is capable of modelling complex roof geometries and separating key building elements relevant for cadastral and valuation purposes. The resulting 3D building model is explicitly structured into assessment-related elements, including roof, exterior walls, and ground surfaces, enabling element-based area computation and cost estimation. This element-wise representation directly supports fiscal cadastral applications by facilitating transparent and consistent property valuation. Quantitative evaluation using point cloud-to-model distance metrics indicates that the roof reconstruction accuracy falls within the commonly reported range for LoD2 building models, although limitations remain due to segmentation precision and the sensitivity of rule-based algorithms to parameter settings. Despite these limitations, the inclusion of exterior wall information, even in limited quantities, significantly improves building envelope alignment and enables the construction of hanging roofs. Overall, the results confirm that the proposed approach provides a feasible solution for 3D building modelling in dense urban environments with constrained data availability, particularly for fiscal cadastral applications.

Acknowledgements

This research is funded by the Indonesian Endowment Fund for Education (LPDP) on behalf of the Indonesian Ministry of

Higher Education, Science and Technology and managed under the EQUITY Program (Contract No. 4298/B3/DT.03.08/2025).

References

B. Souza, G.H., Amorim, A., 2012. LiDAR data integration for 3D cadastre: some experiences from Brazil. FIG Working Week.

Biljecki, F., Ledoux, H., Stoter, J., 2014. Height references of CityGML LOD1 buildings and their influence on applications. ISPRS 3D GeoInfo 2014 Conference. https://doi.org/10.4233/uuid:09d030b5-67d3-467b-babb-5e5ec10f1b38.

Grilli, E., Daniele, A., Bassier, M., Remondino, F., Serafini, L., 2023. Knowledge enhanced neural networks for point cloud semantic segmentation. Remote Sensing, 15(10). https://doi.org/10.3390/rs15102590.

Grilli, E., Menna, F., Remondino, F., 2017. A review of point clouds segmentation and classification algorithms. Int. Arch. Photogramm. Remote Sens. Spatial Inf. Sci., XLII-2/W3, 339–344. https://doi.org/10.5194/isprs-archives-XLII-2-W3-339-2017.

Huang, J., Stoter, J., Peters, R., Nan, L., 2022. City3D: Large-scale building reconstruction from airborne LiDAR point clouds. Remote Sensing, 14(9). https://doi.org/10.3390/rs14092254.

Kang, C., Wang, F., Zong, M., Cheng, Y., Lu, T., 2019. Research on improved region growing point cloud algorithm. Int. Arch. Photogramm. Remote Sens. Spatial Inf. Sci., XLII-3/W10, 153–157. https://doi.org/10.5194/isprs-archives-XLII-3-W10-153-2020.

Kara, A., van Oosterom, P., Kathmann, R., Lemmen, C., 2023. Visualisation and dissemination of 3D valuation units and groups – an LADM valuation information compliant prototype. Land Use Policy, 132, 106829. https://doi.org/10.1016/j.landusepol.2023.106829.

Kaufhold, L., Kada, M., 2025. Generating watertight 3D building models from airborne LiDAR point clouds using detection transformer (DETR). Int. Arch. Photogramm. Remote Sens. Spatial Inf. Sci., XLVIII-G-2025, 773–780. https://doi.org/10.5194/isprs-archives-XLVIII-G-2025-773-2025.

Kim, T., Cho, W., Matono, A., Kim, K.S., 2020. PinSout: automatic 3D indoor space construction from point clouds with deep learning. Proc. ACM Int. Symp. Adv. Geogr. Inf. Syst., 211–214. https://doi.org/10.1145/3397536.3422343.

Kolbe, T.H., Gröger, G., Plümer, L., 2005. CityGML – interoperable access to 3D city models. Symposium on Geo-Information for Disaster Management.

Nan, L., Wonka, P., 2017. PolyFit: polygonal surface reconstruction from point clouds. Proc. IEEE Int. Conf. Comput. Vis.

Oosterom, P. van, Stoter, J., Lemmen, C., 2005. Modelling of 3D cadastral systems. FIG Working Week.

Patil, J., Kalantari, M., 2025. Automatic scan-to-BIM – the impact of semantic segmentation accuracy. Buildings, 15(7). https://doi.org/10.3390/buildings15071126.

Phan, A.V., Nguyen, M.L., Nguyen, Y.L.H., Bui, L.T., 2018. DGCNN: a convolutional neural network over large-scale labeled graphs. Neural Networks, 108, 533–543. https://doi.org/10.1016/j.neunet.2018.09.001.

Qi, C.R., Yi, L., Su, H., Guibas, L.J., 2017. PointNet++: deep hierarchical feature learning on point sets in a metric space. arXiv preprint, arXiv:1706.02413.

Thomas, H., Qi, C.R., Deschaud, J.-E., Marcotegui, B., Goulette, F., Guibas, L.J., 2019. KPConv: flexible and deformable convolution for point clouds. Proc. IEEE Int. Conf. Comput. Vis.

Tokla, S., Subsomboon, K., 2020. BIM-based simplified approach to automatically estimate building costs for projects in Thailand. Int. J. GEOMATE, 18(68), 101–107. https://doi.org/10.21660/2020.68.5777.

Wang, R., Huang, S., Yang, H., 2023. Building3D: an urban-scale dataset and benchmarks for learning roof structures from point clouds. arXiv preprint, arXiv:2307.11914.

Widyastuti, R., Suwardhi, D., Meilano, I., Hernandi, A., Firdaus, J., 2025. Automating three-dimensional cadastral models of 3D rights and buildings based on the LADM framework. ISPRS Int. J. Geo-Inf., 14(8). https://doi.org/10.3390/ijgi14080293.

Widyastuti, R., Suwardhi, D., Meilano, I., Hernandi, A., Putri, N.S.E., Saptari, A.Y., Sudarman, 2024. Performance analysis of random forest algorithm in automatic building segmentation with limited data. ISPRS Int. J. Geo-Inf., 13(7), 235. https://doi.org/10.3390/ijgi13070235.

Yahya, Z., Rahmat, R.W., Khalid, F., Rizaan, A., Rizal, A., 2017. A concave hull based algorithm for object shape reconstruction. Int. J. Inf. Technol. Comput. Sci., 9(3), 1–9. https://doi.org/10.5815/ijitcs.2017.03.01.

Yamani, S. El, Hajji, R., Nys, G.A., Ettarid, M., Billen, R., 2021. 3D variables requirements for property valuation modeling based on the integration of BIM and CIM. Sustainability, 13(5). https://doi.org/10.3390/su13052814.

Yi, C., Zhang, Y., Wu, Q., Xu, Y., Remil, O., Wei, M., Wang, J., 2017. Urban building reconstruction from raw LiDAR point data. Comput. Aided Des., 93, 1–14. https://doi.org/10.1016/j.cad.2017.07.005.

Appendix

The code and example datasets used in this study are available in a public GitHub repository: https://github.com/ratri89/plane-intersection-reconstruction-pcd-3d-buildingmodels.git. This paper refers to the repository version at commit 3acc824 (accessed on 19 January 2026).